Performances of diffusion kurtosis imaging and diffusion tensor imaging in detecting white matter abnormality in schizophrenia

CrossMark

Jiajia Zhu[a,1], Chuanjun Zhuo[b,1], Wen Qin[a], Di Wang[a], Xiaomei Ma[a], Yujing Zhou[a], Chunshui Yu[a,*]

[a]Department of Radiology and Tianjin Key Laboratory of Functional Imaging, Tianjin Medical University General Hospital, Tianjin 300052, China
[b]Tianjin Anning Hospital, Tianjin 300300, China

ARTICLE INFO

ABSTRACT

Diffusion kurtosis imaging (DKI) is an extension of diffusion tensor imaging (DTI), exhibiting improved sensitivity and specificity in detecting developmental and pathological changes in neural tissues. However, little attention was paid to the performances of DKI and DTI in detecting white matter abnormality in schizophrenia. In this study, DKI and DTI were performed in 94 schizophrenia patients and 91 sex- and age-matched healthy controls. White matter integrity was assessed by fractional anisotropy (FA), mean diffusivity (MD), axial diffusivity (AD), radial diffusivity (RD), mean kurtosis (MK), axial kurtosis (AK) and radial kurtosis (RK) of DKI and FA, MD, AD and RD of DTI. Group differences in these parameters were compared using tract-based spatial statistics (TBSS) ($P < 0.01$, corrected). The sensitivities in detecting white matter abnormality in schizophrenia were MK (34%) > AK (20%) > RK (3%) and RD (37%) > FA (24%) > MD (21%) for DKI, and RD (43%) > FA (30%) > MD (21%) for DTI. DKI-derived diffusion parameters (RD, FA and MD) were sensitive to detect abnormality in white matter regions (the corpus callosum and anterior limb of internal capsule) with coherent fiber arrangement; however, the kurtosis parameters (MK and AK) were sensitive to reveal abnormality in white matter regions (the juxtacortical white matter and corona radiata) with complex fiber arrangement. In schizophrenia, the decreased AK suggests axonal damage; however, the increased RD indicates myelin impairment. These findings suggest that diffusion and kurtosis parameters could provide complementary information and they should be jointly used to reveal pathological changes in schizophrenia.

1. Introduction

Diffusion tensor imaging (DTI) is the most commonly used MRI method that has been applied to evaluate white matter changes of the brain (Catani et al., 2002; Mori et al., 2002; Pierpaoli et al., 1996). Among the parameters derived from DTI, the fractional anisotropy (FA), measuring the degree of anisotropy and ranging between 0 (fully isotropic diffusion) and 1 (fully anisotropic diffusion), is the most commonly used parameter of white matter integrity (Beaulieu, 2002; Bennett et al., 2010; Gulani et al., 2001; Le Bihan et al., 2001). The FA reduction has been found in multiple white matter regions in patients with schizophrenia (Abdul-Rahman et al., 2011; Buchsbaum et al., 1998; Ellison-Wright et al., 2014; Ellison-Wright and Bullmore, 2009; Kunimatsu et al., 2012; Kyriakopoulos et al., 2008; Nazeri et al., 2013; Rosenberger et al., 2012). Therefore, schizophrenia is an ideal model to test the sensitivity differences in detecting abnormality in white matter integrity between different imaging methods. In addition, mean

diffusivity (MD), axial diffusivity (AD) and radial diffusivity (RD) can also be calculated from DTI data and reflect different pathological changes in schizophrenia (Budde et al., 2007; Song et al., 2003).

Conventional DTI measures water diffusion based on the assumption that the displacement distribution of water molecule in a given time is a Gaussian function (Basser and Jones, 2002). However, this assumption may not be valid in biological tissues where water molecules often show non-Gaussian diffusion due to the presence of barriers such as cell membranes and organelles (Tuch et al., 2003). Several approaches have been proposed to characterize the non-Gaussian diffusion, such as the Q-space imaging (Assaf et al., 2002a; Assaf et al., 2002b) and diffusion spectrum imaging (Wedeen et al., 2005). However, the application of these techniques as routine clinical protocols has been challenged by its longer scan times and higher hardware demands.

Recently, diffusion kurtosis imaging (DKI) has been proposed to characterize non-Gaussian diffusion by estimating the excess kurtosis of the displacement distribution (Hui et al., 2008; Jensen et al., 2005; Jensen and Helpern, 2010; Lu et al., 2006; Veraart et al., 2011a). Based on DKI data, both diffusion parameters (FA, MD, AD and RD) and kurtosis parameters including mean kurtosis (MK), axial kurtosis (AK) and radial kurtosis (RK) could be obtained (Jensen et al., 2005; Jensen and Helpern, 2010; Lu et al., 2006; Wu and Cheung, 2010). The kurtosis

---

parameters of DKI are especially suitable for evaluating microstructural integrity in white matter regions with complex fiber arrangement (Hori et al., 2012; Lazar et al., 2008; Lu et al., 2006). DKI has exhibited improved sensitivity and specificity in detecting developmental and pathological changes in neural tissues as compared to conventional DTI (Adisetiyo et al., 2014; Blockx et al., 2012a; Blockx et al., 2012b; Cheung et al., 2009; Cheung et al., 2012; Falangola et al., 2008; Gao et al., 2012; Grinberg et al., 2012; Grossman et al., 2012; Helpern et al., 2011; Hui et al., 2012; Jensen et al., 2011; Raab et al., 2010; Van Cauter et al., 2012; Wang et al., 2011; Zhuo et al., 2012). In particular, a pioneer study has compared DKI-derived parameters (MK, FA and MD) in the prefrontal cortex between schizophrenia patients and healthy subjects using a histogram analysis approach (Ramani et al., 2007). A reduction in MK and FA in the white matter of the prefrontal cortex was observed in schizophrenia patients, which suggested a loss of microstructural integrity in this region.

In the present study, we reconstructed the white matter skeleton of the brain using tract-based spatial statistics (TBSS) (Smith et al., 2006) and compared differences in diffusion and kurtosis parameters within the skeleton between schizophrenia patients (n = 94) and healthy controls (n = 91). The aim of this study is to assess the performances of 11 commonly used parameters derived from DKI (MK, AK, RK, FA, MD, AD and RD) and DTI (FA, MD, AD and RD) in detecting white matter abnormality in schizophrenia.

2. Materials and methods

This study was approved by the Ethics Committee of Tianjin Medical University General Hospital, and written informed consent was obtained from each subject before study enrollment. The funding sources for this study had no role in the preparation of the manuscript.

2.1. Subjects

A total of 106 patients with schizophrenia and 94 healthy controls were included in our study. Diagnosis for individual schizophrenia patient was determined by the consensus of two psychiatrists using the Structured Clinical Interview for DSM-IV. Inclusion criteria were age (16–60 years) and right-handedness. Exclusion criteria for all participants were MRI contraindications, pregnancy, and histories of systemic medical illness, central nervous system disorder and head trauma that would affect study results, and substance abuse within the last 3 months or lifetime history of substance abuse or dependence. Additional exclusion criteria for healthy controls were history of any Axis I or II disorders and a psychotic disorder and first-degree relative with a psychotic disorder. After image quality assessment slice by slice by two professional radiologists, 12 patients and 3 healthy controls were excluded due to poor quality of imaging data. The final sample included 94 schizophrenia patients and 91 healthy controls (Table 1). A Chi-square test of Pearson and a t-test of Student were used to test the group differences in sex and age, respectively. There were no significant group differences in sex

Table 1
Demographic and clinical characteristics of schizophrenia patients and healthy controls.

Characteristic	Schizophrenia patients	Healthy controls	P value
Number of subjects	94	91	
Age (years)	33.5 ± 8.4	33.5 ± 10.3	0.947
Sex (female/male)	38/56	46/45	0.167
Antipsychotic dosage (mg/day) (chlorpromazine equivalents)	462.5 ± 346.8	NA	
Duration of illness (months)	123.1 ± 98.6	NA	
PANSS			
Positive score	17.1 ± 7.8	NA	
Negative score	19.5 ± 8.2	NA	

Note: The data were shown as the mean values ± standard deviations. Abbreviations: NA, not applicable; PANSS, The Positive and Negative Syndrome Scale.

($\chi^2 = 1.912$, $P = 0.167$) and age (t = 0.067, $P = 0.947$). Eighty-five patients were receiving atypical antipsychotic medications when performing the MRI examinations and the other 9 patients had never received any medications. Clinical symptoms of psychosis were quantified with the Positive and Negative Syndrome Scale (PANSS) (Kay et al., 1987).

2.2. MRI data acquisition

MRI was performed using a 3.0-Tesla MR system (Discovery MR750, General Electric, Milwaukee, WI, USA). Tight but comfortable foam padding was used to minimize head motion, and earplugs were used to reduce scanner noise. DKI data were acquired by a spin-echo single-shot echo planar imaging (EPI) sequence with the following parameters (Jensen and Helpern, 2010): repetition time = 5800 ms; echo time = 77 ms; matrix = 128 × 128; field of view = 256 × 256 mm; in-plane resolution = 2 × 2 mm; slice thickness = 3 mm without gap; 48 axial slices; 25 encoding diffusion directions with two values of b (b = 1000 and 2000 s/mm^2) for each direction and 10 non-diffusion-weighted images (b = 0 s/mm^2). The total acquisition time for DKI was 5 min and 54 s. All images were visually inspected to ensure only images without visible artifacts were included in subsequent analyses.

2.3. Theoretical models of DTI and DKI

Conventional DTI assumed that the water molecules diffuse freely and unrestrictedly with a Gaussian distribution of diffusion displacement. For a given diffusion-encoding direction, the apparent diffusivity (D_{app}) of water molecules can be calculated by linearly fitting the diffusion-weighted signals acquired with one or more b-values to the following equation (Basser and Jones, 2002; Basser and Pierpaoli, 1996):

$$\ln\frac{S(b)}{S(0)} = -bD_{app}$$

where S(0) is the signal intensity without diffusion weighting and S(b) is the diffusion-weighted signal intensity at a particular b-value. DKI assumed that the diffusion of a water molecule follows a non-Gaussian distribution due to restriction by the tissue microstructure. Differing from conventional DTI, DKI fits the diffusion-weighted signal in a given diffusion direction as a function of the b-value to the following equation (Jensen et al., 2005; Jensen and Helpern, 2010; Lu et al., 2006):

$$\ln\frac{S(b)}{S(0)} = -bD_{app} + \frac{1}{6}b^2 D_{app}^2 K_{app}$$

where D_{app} is the apparent diffusion coefficient and K_{app} is the apparent diffusion kurtosis. With these two tensors, a number of diffusion and kurtosis parameters can be determined.

2.4. Calculation of diffusion and kurtosis parameters

Eddy current-induced distortion and motion artifacts in the DKI dataset were corrected using affine alignment of each diffusion-weighted image to the b = 0 image using FMRIB's diffusion toolbox (FSL 4.0, http://www.fmrib.ox.ac.uk/fsl). After skull-stripping, Diffusional Kurtosis Estimator (http://www.nitrc.org/projects/dke) was implemented to calculate the diffusion and kurtosis tensors using the constrained linear least squares-quadratic programming (CLLS-QP) algorithm as described previously (Tabesh et al., 2011). All the data (b = 0, 1000, 2000 s/mm^2) were used for DKI fitting because DKI parameters (MK, AK, RK, FA, MD, AD and RD) can only be estimated based on at least two non-zero b values in more than 15 independent directions (Hui et al., 2008; Poot et al., 2010). Only images with b = 0 and 1000 s/mm^2 were employed for DTI fitting because DTI parameters (FA, MD, AD and RD) can be estimated using a mono-exponential model based on a single non-zero b value in six independent directions.

2.5. Tract-based spatial statistics

The following steps were adopted for the TBSS analysis (Smith et al., 2006). All subjects' DKI_FA images were aligned to a template of averaged FA images (FMRIB-58) in the Montreal Neurological Institute (MNI) space using a non-linear registration algorithm implemented in FNIRT (FMRIB's Non-linear Registration Tool). After transformation into the MNI space, a mean DKI_FA image was created and thinned to generate a mean DKI_FA skeleton of the white matter tracts. Each subject's DKI_FA image was then projected onto the skeleton via filling the mean DKI_FA skeleton with DKI_FA values from the nearest relevant tract center by searching perpendicular to the local skeleton structure for maximum DKI_FA value. The registration and projection information derived from the DKI_FA analysis were then applied to the other 10 parametric images of each subject to ensure an exact spatial correspondence of the different parameters.

Voxel-wise statistical analysis across subjects on the skeleton space was carried out using a permutation-based inference tool for nonparametric statistic ("randomize", part of FSL). Group comparisons between schizophrenia patients and healthy controls were performed using a general linear model with age and gender as covariates of no interest.

The mean DKI_FA skeleton was used as a mask, and the number of permutations was set to 5000. To simultaneously control for both type I and type II errors, the significance threshold was determined with a $P < 0.01$ (two-tailed) after correcting for family-wise error (FWE) using the threshold-free cluster enhancement (TFCE) (Smith and Nichols, 2009) option in FSL. To facilitate visualization, results were thickened using the tbss_fill script implemented in FSL. Fiber tracts corresponding to the clusters were identified with reference to the Johns Hopkins University ICBM-DTI-81 White-Matter Labels provided in the FSL toolbox. To quantitatively compare the sensitivity of parameters from DKI and DTI in detecting white matter integrity impairments in schizophrenia, we also calculated the percentage of the abnormal voxels relative to the whole skeleton voxels for each parameter.

3. Results

3.1. Kurtosis parameters from DKI

The white matter fibers with significant intergroup differences ($P < 0.01$, two-tailed, FWE corrected) in DKI-derived kurtosis
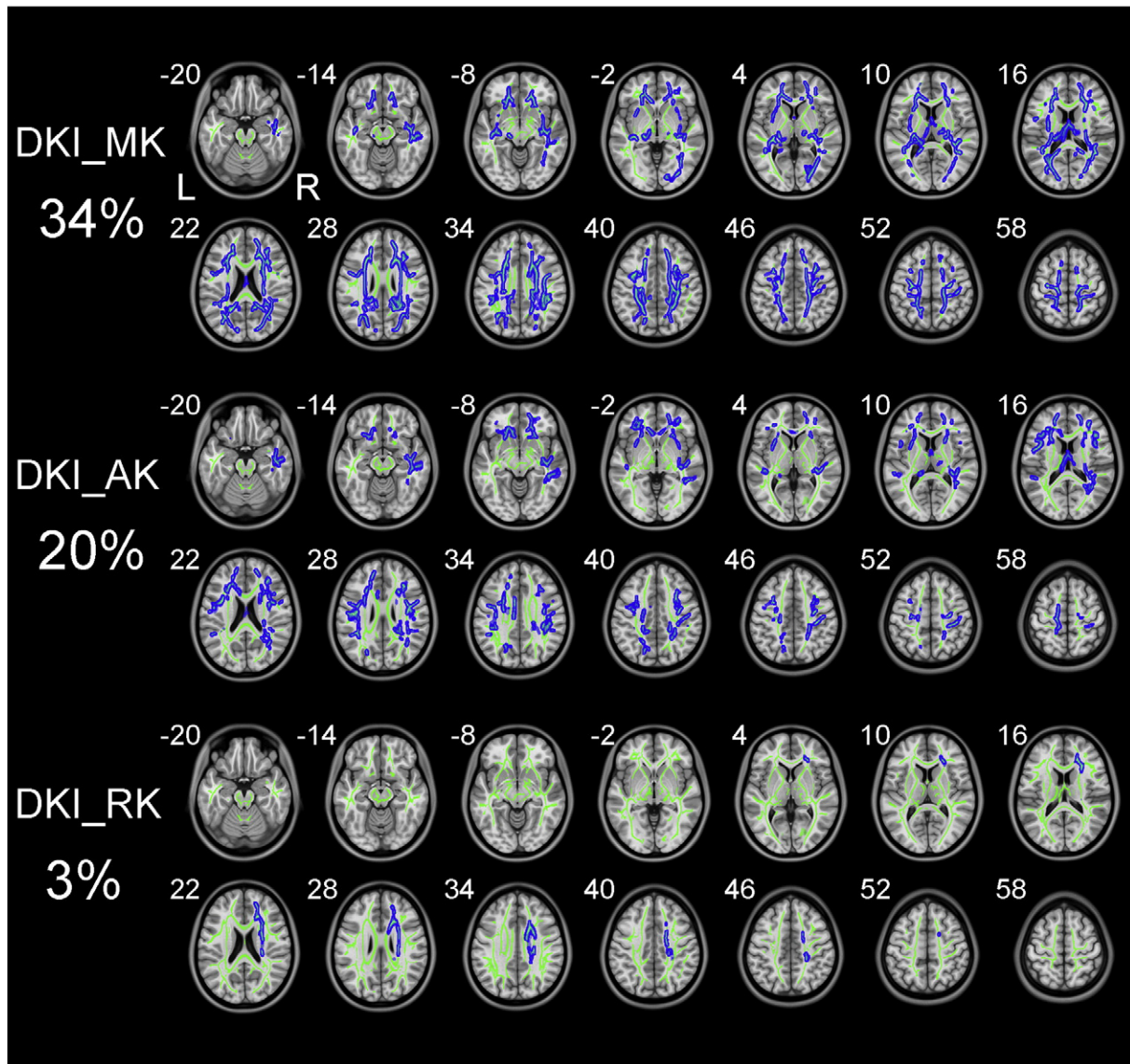

Fig. 1. TBSS shows white matter regions with significant differences in the DKI_MK, DKI_AK and DKI_RK between schizophrenia patients and healthy subjects ($P < .01$, FWE corrected). Green represents mean FA skeleton of all participants; red denotes increase and blue represents reduction in schizophrenia patients. The percentage in the left column represents the percentage of the abnormal voxels relative to the whole skeleton voxels for each parameter.

parameters are shown in Fig. 1. Compared to healthy controls, schizophrenia patients exhibited significantly decreased kurtosis parameters in white matter regions with complex fiber arrangement, such as in the juxtacortical white matter and corona radiata (CR). DKI_MK, DKI_AK and DKI_RK could detect abnormal diffusion in 34%, 20% and 3% voxels of the whole white matter skeleton, respectively.

3.2. Diffusion parameters from DKI

The white matter fibers with significant intergroup differences ($P < 0.01$, two-tailed, FWE corrected) in DKI-derived diffusion parameters are shown in Fig. 2. Compared to healthy controls, schizophrenia patients exhibited reduced DKI_FA in white matter regions with coherent fiber arrangement, such as the corpus callosum (CC) and anterior limb of internal capsule (ALIC). Schizophrenia patients also showed increased DKI_MD and DKI_RD relative to healthy controls. However, there was no significant difference in DKI_AD between the two groups. DKI_RD, DKI_FA and DKI_MD could detect abnormal diffusion in 37%, 24% and 21% voxels of the whole white matter skeleton, respectively.

3.3. Diffusion parameters from DTI

The white matter fibers with significant intergroup differences ($P < 0.01$, two-tailed, FWE corrected) in DTI-derived diffusion parameters are shown in Fig. 3. Similar with changes in DKI-derived diffusion parameters, schizophrenia patients demonstrated reduced FA, increased MD and RD, and unchanged AD when compared to healthy controls. DTI_RD, DTI_FA and DTI_MD could detect abnormal diffusion in 43%, 30% and 21% voxels of the whole white matter skeleton, respectively. More specifically, schizophrenia patients exhibited decreased DTI_FA and increased DTI_RD in widespread white matter regions including the temporal and frontal lobes, CC, ALIC and fornix.

4. Discussion

In our study, extensive white matter impairments were found in schizophrenia patients compared to healthy subjects using both DKI and conventional DTI. We observed that DKI-derived kurtosis and diffusion parameters were sensitive to detect abnormality in white matter
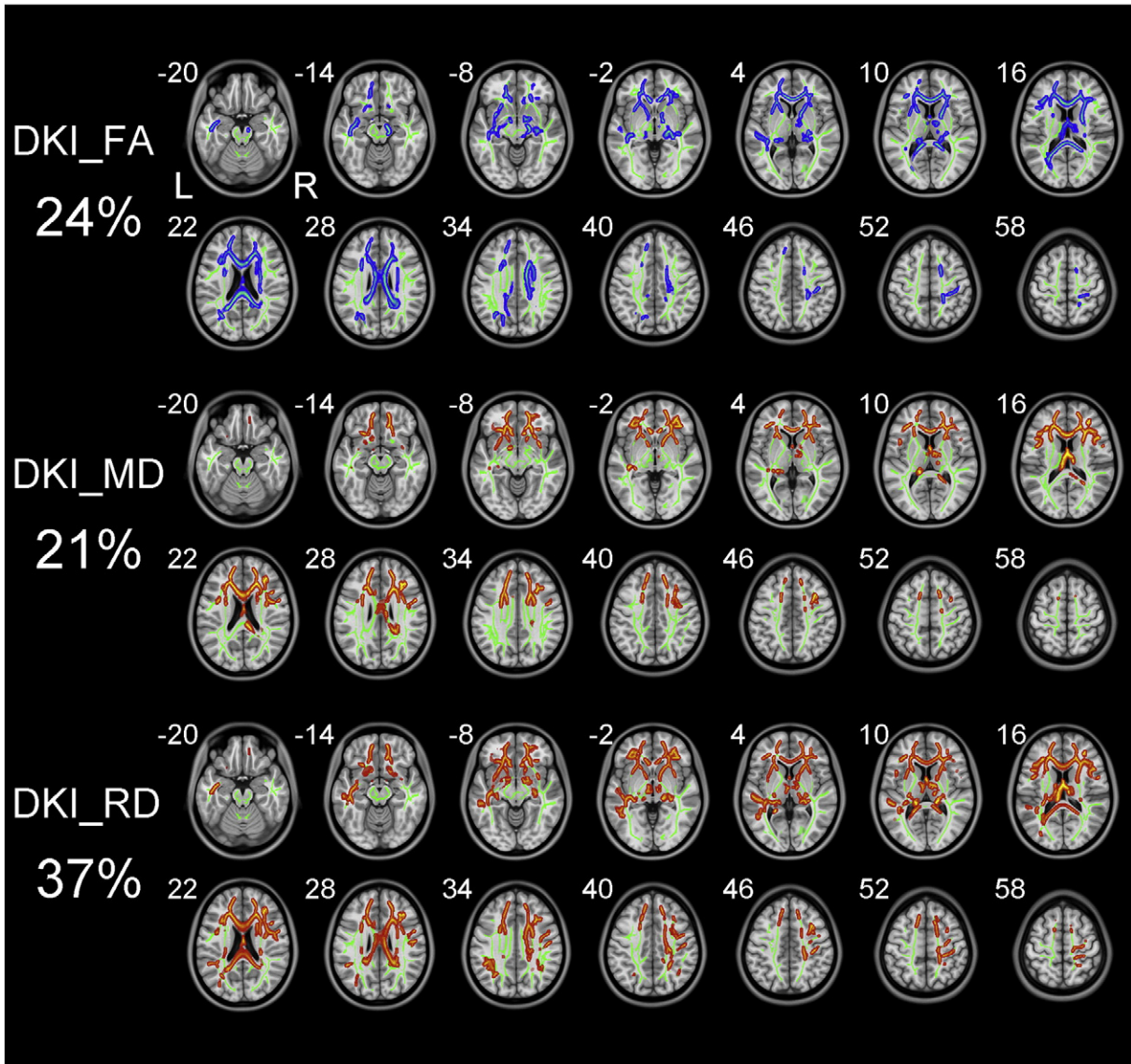

Fig. 2. TBSS shows white matter regions with significant differences in the DKI_FA, DKI_MD and DKI_RD between schizophrenia patients and healthy subjects ($P < .01$, FWE corrected). Green represents mean FA skeleton of all participants; red denotes increase and blue represents reduction in schizophrenia patients. The percentage in the left column represents the percentage of the abnormal voxels relative to the whole skeleton voxels for each parameter.

Fig. 3. TBSS shows white matter regions with significant differences in the DTI_FA, DTI_MD and DTI_RD between schizophrenia patients and healthy subjects ($P < .01$, FWE corrected). Green represents mean FA skeleton of all participants; red denotes increase and blue represents reduction in schizophrenia patients. The percentage in the left column represents the percentage of the abnormal voxels relative to the whole skeleton voxels for each parameter.
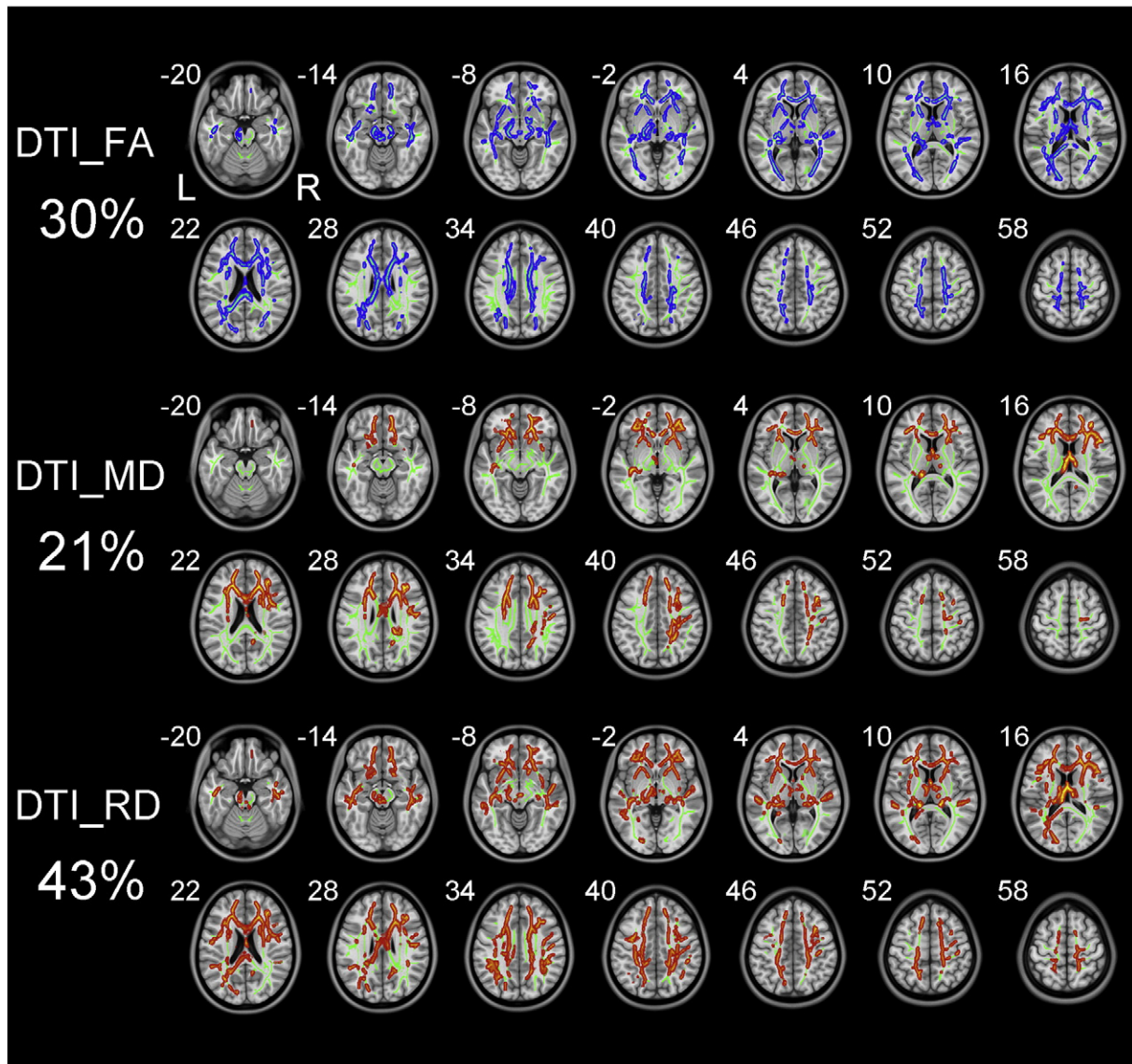
regions with different fiber arrangements. The DKI-derived kurtosis parameters were sensitive to detect abnormality in white matter regions with complex fiber arrangement; however, the DKI-derived diffusion parameters were sensitive to detect abnormality in white matter regions with coherent fiber arrangement. Moreover, the MK decrease in schizophrenia is predominantly driven by the AK decrease; in contrast, the FA decrease is mainly caused by the increase of RD.

The conventional diffusion parameters are estimated by the mono-exponential model, which makes their values depend on the selection of b-values (Veraart et al., 2011a). Because the DTI_FA reflects the mean anisotropy of a voxel, it cannot accurately estimate the anisotropy of white matter voxels with multiple fibers in different directions. As an extension of the DTI model, DKI requires at least two non-zero b values in more than 15 independent directions (Hui et al., 2008; Poot et al., 2010). Using a second-order polynomial model, DKI provides a b-value-independent estimation of the diffusion (Veraart et al., 2011a; Veraart et al., 2011b) and kurtosis parameters (Jensen et al., 2005; Jensen and Helpern, 2010; Lu et al., 2006). Theoretically, DKI is an ideal technique for estimating the restricted diffusion process *in vivo*,

and could be a valuable tool for detecting pathological alterations in neural tissues.

The diffusion and kurtosis parameters measure different characteristics of water diffusion and have different sensitivities in detecting abnormality in white matter regions with different microstructures. As the most commonly used diffusion parameter, the DKI_FA measures directional anisotropy of water molecules in a given voxel and is suitable for assessing white matter regions with coherent fiber arrangement. However, it has limited capacity of detecting diffusion changes in white matter regions with complex fiber arrangement, such as fiber crossing (Douaud et al., 2011; Jbabdi et al., 2010; Vos et al., 2012). The DKI_MK, the most characteristic parameter of DKI, measures the degree to which the diffusion displacement probability distribution is non-Gaussian and is suitable for assessing white matter regions with complex fiber arrangement (Lazar et al., 2008). Therefore, the diffusion and kurtosis parameters are suitable for evaluating different white matter structures and the combination of these two parameters may improve the sensitivity in detecting alterations in white matter integrity in brain disorders. This theoretical prediction has been validated by

our findings that altered diffusion parameters (especially reduced DKI_FA) were mainly located in white matter regions with coherent fiber arrangement, such as the CC and ALIC; however, reduced kurtosis parameters (especially DKI_MK) were observed mainly in white matter regions with complex fiber arrangement, such as the juxtacortical white matter and CR. These findings suggest that researchers should select appropriate DKI parameters to sensitively detect diffusion changes in specific white matter regions in schizophrenia.

In the current study, schizophrenia patients demonstrated lower DTI_FA in widespread white matter regions, especially the temporal and frontal lobes, CC, ALIC and fornix, which are consistent with previous DTI studies (Abdul-Rahman et al., 2011; Ellison-Wright et al., 2014; Ellison-Wright and Bullmore, 2009; Kunimatsu et al., 2012; Kyriakopoulos et al., 2008; Rosenberger et al., 2012). Decreased MK and FA in the white matter of the prefrontal cortex in schizophrenia patients observed in this study are in line with a pioneer study using a histogram analysis approach (Ramani et al., 2007). Among the diffusion parameters derived from either DKI or DTI, the increased RD was the most prominent change in schizophrenia. The increased RD and unchanged AD may suggest myelin abnormalities in schizophrenia, which is in line with previous studies (Lee et al., 2013; Scheel et al., 2013; Seal et al., 2008). In contrast, the MK decrease in schizophrenia is predominantly driven by the decrease of the AK. The reduced AK reflects decreased microstructural complexity along the axial direction of white matter fibers, which may suggest disrupted axonal integrity in schizophrenia (Wu and Cheung, 2010). Therefore, the combination of diffusion and kurtosis parameters, especially directional parameters, may improve our understanding on the pathological changes in schizophrenia.

This study has several limitations that should be addressed in future work. Firstly, we only focused on the capacity of DKI and DTI in detecting abnormality in white matter skeleton reconstructed using the TBSS method; however, their performance differences could be investigated either in white matter regions using an appropriated atlas or in white matter fiber tracts reconstructed by tractography in future studies. Secondly, our study lack correlation analyses between imaging parameters and clinical data, although the primary purpose of this article is to test the feasibility of DKI in schizophrenia researches. Future studies which correlate DKI parameters with clinical characteristics are needed to test whether the DKI can be used as a clinical biomarker although the biophysical property underlying the kurtosis is still not fully understood and needs *ex vivo* validation. Thirdly, we did not collect information of educational levels, which may be different between the two groups and may affect our results. Finally, we did not analyze performances of DKI and DTI in detecting gray matter abnormalities in schizophrenia because previous studies have found significant partial volume effect of cerebrospinal fluid on the diffusion parameters of the gray matter (Hu et al., 2008; Yang et al., 2013). This effect may be more prominent in the significantly atrophic gray matter in schizophrenia (Crow et al., 1980; Weinberger and Wyatt, 1980).

In conclusion, this study demonstrated that the DKI-derived diffusion and kurtosis parameters were sensitive to detect abnormality in white matter regions with different fiber arrangements, which may guide researchers to use an appropriate DKI parameter to detect abnormality in specific white matter regions. We also confirm that the combination of directional diffusion and kurtosis parameters could provide more directionally specific and complementary information, which may improve our understanding on the underlying pathological changes in schizophrenia. These findings suggest that multiple diffusion and kurtosis parameters should be jointly used to reveal pathological changes in schizophrenia.

Acknowledgments

References

Abdul-Rahman, M.F., Qiu, A., Sim, K., 2011. Regionally specific white matter disruptions of fornix and cingulum in schizophrenia. PLOS One 6 (4), e18652. http://dx.doi.org/10.1371/journal.pone.001865221533181.

Adisetiyo, V., Tabesh, A., Di Martino, A., Falangola, M.F., Castellanos, F.X., Jensen, J.H., Helpern, J.A., 2014. Attention-deficit/hyperactivity disorder without comorbidity is associated with distinct atypical patterns of cerebral microstructural development. Hum. Brain Mapp. 35 (5), 2148–2162. http://dx.doi.org/10.1002/hbm.2231723907808.

Assaf, Y., Ben-Bashat, D., Chapman, J., Peled, S., Biton, I.E., Kafri, M., Segev, Y., Hendler, T., Korczyn, A.D., Graif, M., Cohen, Y., 2002a. High b-value q-space analyzed diffusion-weighted MRI: application to multiple sclerosis. Magn. Reson. Med. 47 (1), 115–126. http://dx.doi.org/10.1002/mrm.1004011754450.

Assaf, Y., Mayzel-Oreg, O., Gigi, A., Ben-Bashat, D., Mordohovitch, M., Verchovsky, R., Reider-Groswasser, I.I., Hendler, T., Graif, M., Cohen, Y., Korczyn, A.D., 2002b. High b value q-space-analyzed diffusion MRI in vascular dementia: a preliminary study. J. Neurol. Sci. 203–204, 235–239. http://dx.doi.org/10.1016/S0022-510X(02)00297-6.

Basser, P.J., Jones, D.K., 2002. Diffusion-tensor MRI: theory, experimental design and data analysis — a technical review. NMR Biomed. 15 (7–8), 456–467. http://dx.doi.org/10.1002/nbm.78312489095.

Basser, P.J., Pierpaoli, C., 1996. Microstructural and physiological features of tissues elucidated by quantitative-diffusion-tensor MRI. J. Magn. Reson. B 111 (3), 209–219. http://dx.doi.org/10.1006/jmrb.1996.00868661285.

Beaulieu, C., 2002. The basis of anisotropic water diffusion in the nervous system — a technical review. NMR Biomed. 15 (7–8), 435–455. http://dx.doi.org/10.1002/nbm.78212489094.

Bennett, I.J., Madden, D.J., Vaidya, C.J., Howard, D.V., Howard Jr., J.H., 2010. Age-related differences in multiple measures of white matter integrity: a diffusion tensor imaging study of healthy aging. Hum. Brain Mapp. 31 (3), 378–390. http://dx.doi.org/10.1002/hbm.2087219662658.

Blockx, I., De Groof, G., Verhoye, M., Van Audekerke, J., Raber, K., Poot, D., Sijbers, J., Osmand, A.P., Von Hörsten, S., Van der Linden, A., 2012a. Microstructural changes observed with DKI in a transgenic Huntington rat model: evidence for abnormal neurodevelopment. Neuroimage 59 (2), 957–967. http://dx.doi.org/10.1016/j.neuroimage.2011.08.062.

Blockx, I., Verhoye, M., Van Audekerke, J., Bergwerf, I., Kane, J.X., Delgado y Palacios, R., Veraart, J., Jeurissen, B., Raber, K., von Hörsten, S., Ponsaerts, P., Sijbers, J., Leergaard, T.B., Van der Linden, A., 2012b. Identification and characterization of Huntington related pathology: an in vivo DKI imaging study. Neuroimage 63 (2), 653–662. http://dx.doi.org/10.1016/j.neuroimage.2012.06.032.

Buchsbaum, M.S., Tang, C.Y., Peled, S., Gudbjartsson, H., Lu, D., Hazlett, E.A., Downhill, J., Haznedar, M., Fallon, J.H., Atlas, S.W., 1998. MRI white matter diffusion anisotropy and PET metabolic rate in schizophrenia. Neuroreport 9 (3), 425–430. http://dx.doi.org/10.1097/00001756-199802160-000139512384.

Budde, M.D., Kim, J.H., Liang, H.F., Schmidt, R.E., Russell, J.H., Cross, A.H., Song, S.K., 2007. Toward accurate diagnosis of white matter pathology using diffusion tensor imaging. Magn. Reson. Med. 57 (4), 688–695. http://dx.doi.org/10.1002/mrm.2120017390365.

Catani, M., Howard, R.J., Pajevic, S., Jones, D.K., 2002. Virtual in vivo interactive dissection of white matter fasciculi in the human brain. Neuroimage 17 (1), 77–94. http://dx.doi.org/10.1006/nimg.2002.113612482069.

Cheung, J.S., Wang, E., Lo, E.H., Sun, P.Z., 2012. Stratification of heterogeneous diffusion MRI ischemic lesion with kurtosis imaging: evaluation of mean diffusion and kurtosis MRI mismatch in an animal model of transient focal ischemia. Stroke 43 (8), 2252–2254. http://dx.doi.org/10.1161/STROKEAHA.112.66192622773558.

Cheung, M.M., Hui, E.S., Chan, K.C., Helpern, J.A., Qi, L., Wu, E.X., 2009. Does diffusion kurtosis imaging lead to better neural tissue characterization? A rodent brain maturation study. Neuroimage 45 (2), 386–392. http://dx.doi.org/10.1016/j.neuroimage.2008.12.01819150655.

Crow, T.J., Frith, C.D., Johnstone, E.C., Owens, D.G., 1980. Schizophrenia and cerebral atrophy. Lancet 1 (8178), 1129–1130. http://dx.doi.org/10.1016/S0140-6736(80)91569-X6103453.

Douaud, G., Jbabdi, S., Behrens, T.E., Menke, R.A., Gass, A., Monsch, A.U., Rao, A., Whitcher, B., Kindlmann, G., Matthews, P.M., Smith, S., 2011. DTI measures in crossing-fibre areas: increased diffusion anisotropy reveals early white matter alteration in MCI and mild Alzheimer's disease. Neuroimage 55 (3), 880–890. http://dx.doi.org/10.1016/j.neuroimage.2010.12.00821182970.

Ellison-Wright, I., Bullmore, E., 2009. Meta-analysis of diffusion tensor imaging studies in schizophrenia. Schizophr. Res. 108 (1–3), 3–10. http://dx.doi.org/10.1016/j.schres.2008.11.02119128945.

Ellison-Wright, I., Nathan, P.J., Bullmore, E.T., Zaman, R., Dudas, R.B., Agius, M., Fernandez-Egea, E., Müller, U., Dodds, C.M., Forde, N.J., Scanlon, C., Leemans, A., McDonald, C., Cannon, D.M., 2014. Distribution of tract deficits in schizophrenia. BMC Psychiatry 14, 99. http://dx.doi.org/10.1186/1471-244X-14-9924693962.

Falangola, M.F., Jensen, J.H., Babb, J.S., Hu, C., Castellanos, F.X., Di Martino, A., Ferris, S.H., Helpern, J.A., 2008. Age-related non-Gaussian diffusion patterns in the prefrontal brain. J. Magn. Reson. Imaging 28 (6), 1345–1350. http://dx.doi.org/10.1002/jmri.2160419025941.

Gao, Y., Zhang, Y., Wong, C.S., Wu, P.M., Zhang, Z., Gao, J., Qiu, D., Huang, B., 2012. Diffusion abnormalities in temporal lobes of children with temporal lobe epilepsy: a preliminary diffusional kurtosis imaging study and comparison with diffusion tensor

imaging. NMR Biomed. 25 (12), 1369–1377. http://dx.doi.org/10.1002/nbm.280922674871.

Grinberg, F., Ciobanu, L., Farrher, E., Shah, N.J., 2012. Diffusion kurtosis imaging and log-normal distribution function imaging enhance the visualisation of lesions in animal stroke models. NMR Biomed. 25 (11), 1295–1304. http://dx.doi.org/10.1002/nbm.280222461260.

Grossman, E.J., Ge, Y., Jensen, J.H., Babb, J.S., Miles, L., Reaume, J., Silver, J.M., Grossman, R.I., Inglese, M., 2012. Thalamus and cognitive impairment in mild traumatic brain injury: a diffusional kurtosis imaging study. J. Neurotrauma 29 (13), 2318–2327. http://dx.doi.org/10.1089/neu.2011.176321639753.

Gulani, V., Webb, A.G., Duncan, I.D., Lauterbur, P.C., 2001. Apparent diffusion tensor measurements in myelin-deficient rat spinal cords. Magn. Reson. Med. 45 (2), 191–195. http://dx.doi.org/10.1002/1522-2594(200102)45:2<191::AID-MRM1025>3.0.CO;2-911180424.

Helpern, J.A., Adisetiyo, V., Falangola, M.F., Hu, C., Di Martino, A., Williams, K., Castellanos, F.X., Jensen, J.H., 2011. Preliminary evidence of altered gray and white matter microstructural development in the frontal lobe of adolescents with attention-deficit hyperactivity disorder: a diffusional kurtosis imaging study. J. Magn. Reson. Imaging 33 (1), 17–23. http://dx.doi.org/10.1002/jmri.2239721182116.

Hori, M., Fukunaga, I., Masutani, Y., Taoka, T., Kamagata, K., Suzuki, Y., Aoki, S., 2012. Visualizing non-Gaussian diffusion: clinical application of q-space imaging and diffusional kurtosis imaging of the brain and spine. Magn. Reson. Med. Sci. 11 (4), 221–23323269009.

Hu, C., Jensen, J.H., Falangola, M.F., Helpern, J.A., 2008. CSF Partial Volume Effect for Diffusional Kurtosis Imaging. Proceedings of the 16th Annual Meeting of ISMRM, Toronto, Canada.

Hui, E.S., Cheung, M.M., Qi, L., Wu, E.X., 2008. Towards better MR characterization of neural tissues using directional diffusion kurtosis analysis. Neuroimage 42 (1), 122–134. http://dx.doi.org/10.1016/j.neuroimage.2008.04.23718524628.

Hui, E.S., Du, F., Huang, S., Shen, Q., Duong, T.Q., 2012. Spatiotemporal dynamics of diffusional kurtosis, mean diffusivity and perfusion changes in experimental stroke. Brain Res. 1451, 100–109. http://dx.doi.org/10.1016/j.brainres.2012.02.04422444274.

Jbabdi, S., Behrens, T.E., Smith, S.M., 2010. Crossing fibres in tract-based spatial statistics. Neuroimage 49 (1), 249–256. http://dx.doi.org/10.1016/j.neuroimage.2009.08.03919712743.

Jensen, J.H., Falangola, M.F., Hu, C., Tabesh, A., Rapalino, O., Lo, C., Helpern, J.A., 2011. Preliminary observations of increased diffusional kurtosis in human brain following recent cerebral infarction. NMR Biomed. 24 (5), 452–457. http://dx.doi.org/10.1002/nbm.161020960579.

Jensen, J.H., Helpern, J.A., 2010. MRI quantification of non-Gaussian water diffusion by kurtosis analysis. NMR Biomed. 23 (7), 698–710. http://dx.doi.org/10.1002/nbm.151820632416.

Jensen, J.H., Helpern, J.A., Ramani, A., Lu, H., Kaczynski, K., 2005. Diffusional kurtosis imaging: the quantification of non-Gaussian water diffusion by means of magnetic resonance imaging. Magn. Reson. Med. 53 (6), 1432–1440. http://dx.doi.org/10.1002/mrm.2050815906300.

Kay, S.R., Fiszbein, A., Opler, L.A., 1987. The positive and negative syndrome scale (PANSS) for schizophrenia. Schizophr. Bull. 13 (2), 261–276. http://dx.doi.org/10.1093/schbul/13.2.2613616518.

Kunimatsu, N., Aoki, S., Kunimatsu, A., Abe, O., Yamada, H., Masutani, Y., Kasai, K., Yamasue, H., Ohtomo, K., 2012. Tract-specific analysis of white matter integrity disruption in schizophrenia. Psychiatry Res. 201 (2), 136–143. http://dx.doi.org/10.1016/j.pscychresns.2011.07.01022398298.

Kyriakopoulos, M., Bargiotas, T., Barker, G.J., Frangou, S., 2008. Diffusion tensor imaging in schizophrenia. Eur. Psychiatry 23 (4), 255–273. http://dx.doi.org/10.1016/j.eurpsy.2007.12.00418524546.

Lazar, M., Jensen, J.H., Xuan, L., Helpern, J.A., 2008. Estimation of the orientation distribution function from diffusional kurtosis imaging. Magn. Reson. Med. 60 (4), 774–781. http://dx.doi.org/10.1002/mrm.2172518816827.

Le Bihan, D., Mangin, J.F., Poupon, C., Clark, C.A., Pappata, S., Molko, N., Chabriat, H., 2001. Diffusion tensor imaging: concepts and applications. J. Magn. Reson. Imaging 13 (4), 534–546. http://dx.doi.org/10.1002/jmri.107611276097.

Lee, S.H., Kubicki, M., Asami, T., Seidman, L.J., Goldstein, J.M., Mesholam-Gately, R.I., McCarley, R.W., Shenton, M.E., 2013. Extensive white matter abnormalities in patients with first-episode schizophrenia: a diffusion tensor imaging (DTI) study. Schizophr. Res. 143 (2–3), 231–238. http://dx.doi.org/10.1016/j.schres.2012.11.02923290268.

Lu, H., Jensen, J.H., Ramani, A., Helpern, J.A., 2006. Three-dimensional characterization of non-Gaussian water diffusion in humans using diffusion kurtosis imaging. NMR Biomed. 19 (2), 236–247. http://dx.doi.org/10.1002/nbm.102016521095.

Mori, S., Kaufmann, W.E., Davatzikos, C., Stieltjes, B., Amodei, L., Fredericksen, K., Pearlson, G.D., Melhem, E.R., Solaiyappan, M., Raymond, G.V., Moser, H.W., van Zijl, P.C., 2002. Imaging cortical association tracts in the human brain using diffusion-tensor-based axonal tracking. Magn. Reson. Med. 47 (2), 215–223. http://dx.doi.org/10.1002/mrm.1007411810663.

Nazeri, A., Chakravarty, M.M., Felsky, D., Lobaugh, N.J., Rajji, T.K., Mulsant, B.H., Voineskos, A.N., 2013. Alterations of superficial white matter in schizophrenia and relationship to cognitive performance. Neuropsychopharmacology 38 (10), 1954–1962. http://dx.doi.org/10.1038/npp.2013.9323591167.

Pierpaoli, C., Jezzard, P., Basser, P.J., Barnett, A., Di Chiro, G., 1996. Diffusion tensor MR imaging of the human brain. Radiology 201 (3), 637–648. http://dx.doi.org/10.1148/radiology.201.3.89392098939209.

Poot, D.H., den Dekker, A.J., Achten, E., Verhoye, M., Sijbers, J., 2010. Optimal experimental design for diffusion kurtosis imaging. IEEE Trans. Med. Imaging 29 (3), 819–829. http://dx.doi.org/10.1109/TMI.2009.203791520199917.

Raab, P., Hattingen, E., Franz, K., Zanella, F.E., Lanfermann, H., 2010. Cerebral gliomas: diffusional kurtosis imaging analysis of microstructural differences. Radiology 254 (3), 876–881. http://dx.doi.org/10.1148/radiol.0909081920089718.

Ramani, A., Jensen, J.H., Szulc, K.U., Ali, O., Hu, C., Lu, H., Brodie, J.D., Helpern, J.A., 2007. Assessment of Abnormalities in the Cerebral Microstructure of Schizophrenia Patients: A Diffusional Kurtosis Imaging Study. Proceedings of the 15th Annual Meeting of ISMRM, Berlin, Germany.

Rosenberger, G., Nestor, P.G., Oh, J.S., Levitt, J.J., Kindleman, G., Bouix, S., Fitzsimmons, J., Niznikiewicz, M., Westin, C.F., Kikinis, R., McCarley, R.W., Shenton, M.E., Kubicki, M., 2012. Anterior limb of the internal capsule in schizophrenia: a diffusion tensor tractography study. Brain Imaging Behav. 6 (3), 417–425. http://dx.doi.org/10.1007/s11682-012-9152-922415192.

Scheel, M., Prokscha, T., Bayerl, M., Gallinat, J., Montag, C., 2013. Myelination deficits in schizophrenia: evidence from diffusion tensor imaging. Brain Struct. Funct. 218 (1), 151–156. http://dx.doi.org/10.1007/s00429-012-0389-222327232.

Seal, M.L., Yücel, M., Fornito, A., Wood, S.J., Harrison, B.J., Walterfang, M., Pell, G.S., Pantelis, C., 2008. Abnormal white matter microstructure in schizophrenia: a voxelwise analysis of axial and radial diffusivity. Schizophr. Res. 101 (1–3), 106–110. http://dx.doi.org/10.1016/j.schres.2007.12.48918262770.

Smith, S.M., Jenkinson, M., Johansen-Berg, H., Rueckert, D., Nichols, T.E., Mackay, C.E., Watkins, K.E., Ciccarelli, O., Cader, M.Z., Matthews, P.M., Behrens, T.E., 2006. Tract-based spatial statistics: voxelwise analysis of multi-subject diffusion data. Neuroimage 31 (4), 1487–1505. http://dx.doi.org/10.1016/j.neuroimage.2006.02.02416624579.

Smith, S.M., Nichols, T.E., 2009. Threshold-free cluster enhancement: addressing problems of smoothing, threshold dependence and localisation in cluster inference. Neuroimage 44 (1), 83–98. http://dx.doi.org/10.1016/j.neuroimage.2008.03.06118501637.

Song, S.K., Sun, S.W., Ju, W.K., Lin, S.J., Cross, A.H., Neufeld, A.H., 2003. Diffusion tensor imaging detects and differentiates axon and myelin degeneration in mouse optic nerve after retinal ischemia. Neuroimage 20 (3), 1714–1722. http://dx.doi.org/10.1016/j.neuroimage.2003.07.00514642481.

Tabesh, A., Jensen, J.H., Ardekani, B.A., Helpern, J.A., 2011. Estimation of tensors and tensor-derived measures in diffusional kurtosis imaging. Magn. Reson. Med. 65 (3), 823–836. http://dx.doi.org/10.1002/mrm.2265521337412.

Tuch, D.S., Reese, T.G., Wiegell, M.R., Wedeen, V.J., 2003. Diffusion MRI of complex neural architecture. Neuron 40 (5), 885–895. http://dx.doi.org/10.1016/S0896-6273(03)00758-X14659088.

Van Cauter, S., Veraart, J., Sijbers, J., Peeters, R.R., Himmelreich, U., De Keyzer, F., Van Gool, S.W., Van Calenbergh, F., De Vleeschouwer, S., Van Hecke, W., Sunaert, S., 2012. Gliomas: diffusion kurtosis MR imaging in grading. Radiology 263 (2), 492–501. http://dx.doi.org/10.1148/radiol.1211092722403168.

Veraart, J., Poot, D.H., Van Hecke, W., Blockx, I., Van der Linden, A., Verhoye, M., Sijbers, J., 2011a. More accurate estimation of diffusion tensor parameters using diffusion kurtosis imaging. Magn. Reson. Med. 65 (1), 138–145. http://dx.doi.org/10.1002/mrm.2260320878760.

Veraart, J., Van Hecke, W., Sijbers, J., 2011b. Constrained maximum likelihood estimation of the diffusion kurtosis tensor using a Rician noise model. Magn. Reson. Med. 66 (3), 678–686. http://dx.doi.org/10.1002/mrm.2283521416503.

Vos, S.B., Jones, D.K., Jeurissen, B., Viergever, M.A., Leemans, A., 2012. The influence of complex white matter architecture on the mean diffusivity in diffusion tensor MRI of the human brain. Neuroimage 59 (3), 2208–2216. http://dx.doi.org/10.1016/j.neuroimage.2011.09.08622005591.

Wang, J.J., Lin, W.Y., Lu, C.S., Weng, Y.H., Ng, S.H., Wang, C.H., Liu, H.L., Hsieh, R.H., Wan, Y.L., Wai, Y.Y., 2011. Parkinson disease: diagnostic utility of diffusion kurtosis imaging. Radiology 261 (1), 210–217. http://dx.doi.org/10.1148/radiol.1110227721771952.

Wedeen, V.J., Hagmann, P., Tseng, W.Y., Reese, T.G., Weisskoff, R.M., 2005. Mapping complex tissue architecture with diffusion spectrum magnetic resonance imaging. Magn. Reson. Med. 54 (6), 1377–1386. http://dx.doi.org/10.1002/mrm.2064216247738.

Weinberger, D.R., Wyatt, R.J., 1980. Schizophrenia and cerebral atrophy. Lancet 1 (8178), 11306103454.

Wu, E.X., Cheung, M.M., 2010. MR diffusion kurtosis imaging for neural tissue characterization. NMR Biomed. 23 (7), 836–848. http://dx.doi.org/10.1002/nbm.150620623793.

Yang, A.W., Jensen, J.H., Hu, C.C., Tabesh, A., Falangola, M.F., Helpern, J.A., 2013. Effect of cerebral spinal fluid suppression for diffusional kurtosis imaging. J. Magn. Reson. Imaging 37 (2), 365–371. http://dx.doi.org/10.1002/jmri.2384023034866.

Zhuo, J., Xu, S., Proctor, J.L., Mullins, R.J., Simon, J.Z., Fiskum, G., Gullapalli, R.P., 2012. Diffusion kurtosis as an in vivo imaging marker for reactive astrogliosis in traumatic brain injury. Neuroimage 59 (1), 467–477. http://dx.doi.org/10.1016/j.neuroimage.2011.07.05021835250.